Comprehensive analysis of temperature rise generated by a titanium rod inside 1.5T MRI RF whole body coil

Mikhail Kozlov[1,2] and Gregor Schaefers[1]
[1]MR:comp GmbH, Gelsenkirchen, North Rhine Westphalia, Germany, [2]MPI, Leipzig, Saxony, Germany

Introduction: ISO/TS 10974 edition 1 [1] and ASTM F2182-11a [2] define test methods for active and passive implants. In both document 10 cm long rod of 3.125 mm in diameter made from Grade 5 high strength titanium is used as tools to estimate or to validate local SAR deposition. However there is no literature data how temperate rise due to presence of the titanium rod depends on location of the rod inside a phantom and 3D EM and temperature simulation simplifications.

Our numerical simulation goals in this study were: a) to evaluate the influence of rod position on the induced temperature rise normalized to incident tangential electric field ($\boldsymbol{T}_{\mathbf{rise}}$), b) to evaluate peak-to-peak variation of the $\boldsymbol{T}_{\mathbf{rise}}$ inside at a set of sub-volumes with 1×1×1 mm dimension, and c) to analyze 3D EM and temperature simulation simplification consequences.

Method: We investigated a locally shielded 64 MHz high pass 16 rung birdcage coils with dimension relevant to clinical 1.5T scanners: coils of diameter 704 mm and length 650 mm. To mimic the clinical case, the coil was tuned and matched when loaded by ANSYS human multi tissue model, temperature rise was evaluated in rectangular (650×420×90 mm) ASTM phantom, located symmetrically to coil centre. Phantom liquid relative electric permittivity was 78 and conductivity was 0.47 S/m. The ANSYS HFSS 2014 was chosen as the 3D EM tool, and thermal solver utilized is part of ANSYS NLT package. 3D EM results were obtained with frequency domain solver convergence $\Delta S<0.002$. Flux convergence of the thermal solver was 1.e-4. Mesh was generated in each solver independently to ensure the best suitable mesh for a given simulation modality. Variable mesh size in area of hot spot was less than 0.1 mm.

The rod, simulated as titanium alloy in both solvers, was located at two positions by defining its shift in X (by 190 and 150 mm) direction from coil centre. In vertical direction the rod was always located in middle of the ASTM phantom. One-mm in diameter holes were centered 1 mm from each end of the rod. A 0.65 mm in diameter fiber glass, located vertically, mimicked use of thermal probe during actual measurement (Fig. 1a). Thermal properties of the ASTM liquid (specific heat was 4182 J× kg^{-1}×K^{-1} and thermal conductivity was 0.6 W×m^{-1}×K^{-1}) and the titanium alloy (specific heat was 522 J× kg^{-1}×K^{-1} and thermal conductivity was 21.9 W×m^{-1}×K^{-1}) were obtained from ANSYS solver material database. Thermal simulation time was 900s. The $\boldsymbol{T}_{\mathbf{rise}}$ was calculated as a difference of temperature rise for cases with and without the rod. For quantitative comparison all results were scaled to average (over location of the rod) incident tangential electrical field of 1V/m.

The following abbreviations are subsequently used for convenience: "***l*×*s***" denotes a simulation setup where ***l*** is the rod shift in X, ***s*** coded a simulation simplification: "***full***"; "***no_glass***" when the fiber glass was not taken into account; "***no_holes***" when the holes were not taken into account. Numbering of sub-volumes of ASTM phantom liquid is given on Fig. 1a. Fiber glass or ASTM phantom liquid (when the fiber glass was not taken into account) sub-volume with 0.4×0.4×0.4 mm dimension and centered in middle of the hole denoted as sensor "***hole***". The value for global max of $\boldsymbol{T}_{\mathbf{rise}}$ presented in column "***peak***".

Results and discussion: Each cell of Table 1 contains two values: the first representing the max $\boldsymbol{T}_{\mathbf{rise}}$ inside sub-volume, expressed in $mK/(V/m)^2$, and the second reporting peak-to-peak variation of the $\boldsymbol{T}_{\mathbf{rise}}$ in %. $\boldsymbol{T}_{\mathbf{rise}}$ was found to be dependent on shift in X direction. There is noticeable influence of fiber glass on power loss density (PLD) profile (Fig.1b) in vicinity of fiber glass and $\boldsymbol{T}_{\mathbf{rise}}$ of sub-volumes located in proximity of rod tip. Expectedly there is no power deposition inside the holes (Fig. 1c). Thus temperature sensor located inside the hole reports temperature rise generated by surrounding media. Because thermal conductivity of titanium alloy is significantly higher the temperature inside hole followed temperature of rod tip with some time delay. In all simulation $\boldsymbol{T}_{\mathbf{rise}}$ of rod tip was found noticeable less than maximum $\boldsymbol{T}_{\mathbf{rise}}$ in ASTM liquid. The current investigation is limited regarding uncertainty of temperature results reported by a thermal probe because the entire thermal probe was simulated as object with thermal properties of the fiber glass. However results for simulation without fiber glass provided strong evidence that $\boldsymbol{T}_{\mathbf{rise}}$ inside hole is less than max $\boldsymbol{T}_{\mathbf{rise}}$ and $\boldsymbol{T}_{\mathbf{rise}}$ for the first sub-volume. For time step 900 s, essential peak-to-peak variation of $\boldsymbol{T}_{\mathbf{rise}}$ inside sub-volumes was observed for all sub-volumes located outside the hole. This variation was as much as twice higher for time step 100 s. Thus position of temperature sensor should be known with sub millimeter precision, to maintain $\boldsymbol{T}_{\mathbf{rise}}$ measurement uncertainty small. It should be noted that thermal conductivity of titanium alloy used in our investigation is significantly higher thermal conductivity of ASTM B348-5 titanium alloy 7.2 W×m^{-1}×K^{-1}, therefore no comparison for published results for ASTM B348-5 titanium alloy was done.

Conclusion: ASTM F2182-11a considers locating an implant 2 cm from the phantom wall as appropriate because 'this location provides a high uniform tangential electric field over a length of approximately 15 cm'. However our finding that $\boldsymbol{T}_{\mathbf{rise}}$ depend on distance to the phantom wall raised a doubt that ASTM F2182-11a suggested position of an implant inside a phantom is sufficient for reliable RF-induced heating investigation. Influence of fiber glass temperature probe on power deposition and temperature rise in vicinity of the probe should be taken into account when uncertainty budget is considered.

Table 1. The $\boldsymbol{T}_{\mathbf{rise}}$ for different rod positions and simulation simplifications

Setup	#1	#2	#3	#4	#5	#6	#7	#8	***hole***	***peak***
190×full	0.234/14.5	0.214/15.7	0.220/15.8	0.217/16.2	0.178/15.1	0.165/15.7	0.171/16.5	0.167/16.7	0.218/0.3	0.248
190×no_glass	0.239/15.0	0.218/16.2	0.224/16.3	0.221/16.6	0.181/15.4	0.167/16.0	0.173/16.8	0.170/16.9	0.232/1.4	0.249
190×no_holes	0.238/14.8	0.218/16.1	0.224/16.2	0.221/16.6	0.181/15.4	0.167/16.0	0.173/16.8	0.170/16.9	-	0.248
150×full	0.268/15.0	0.248/16.1	0.253/16.4	0.251/16.8	0.202/15.8	0.197/15.9	0.187/17.9	0.193/17.5	0.254/0.2	0.286
150×no_glass	0.273/15.7	0.253/16.7	0.258/17.0	0.255/17.3	0.205/16.1	0.200/16.2	0.190/18.3	0.195/17.3	0.270/1.2	0.287
150×no_holes	0.272/15.5	0.252/16.7	0.257/17.0	0.255/17.4	0.204/15.9	0.199/16.1	0.189/18.1	0.195/17.7	-	0.285

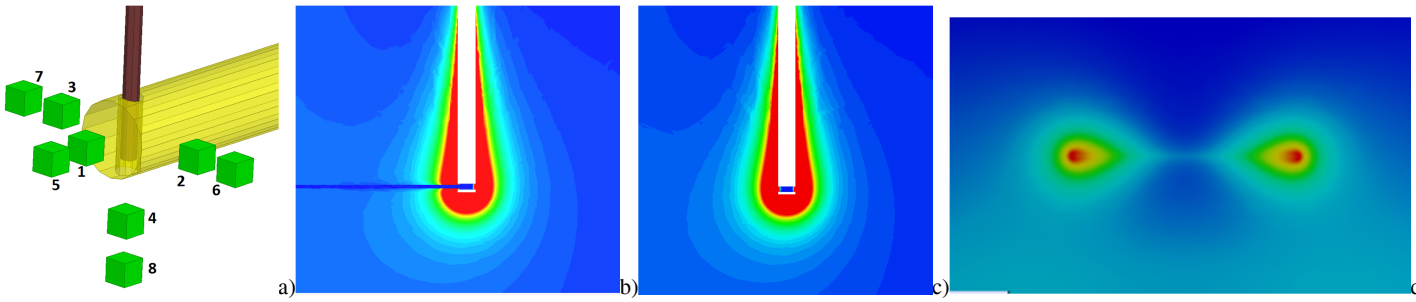

Fig.1. a) location of sub-volumes; b) PLD profile for ***150×full***, c) PLD profile for ***150×no_glass***; d) temperature profile. All profiles plotted in linear scale

[1] Technical specification ISO/TS 10974 "Assessment of the safety of magnetic resonance imaging for patients with an active implantable medical device" 1st edition 2012. [2] F2182 – 11a "Standard Test Method for Measurement of Radio Frequency Induced Heating On or Near Passive Implants During Magnetic Resonance Imaging".